

Phosphorus, Sulfur, and Silicon and the Related Elements

ISSN: 1042-6507 (Print) 1563-5325 (Online) Journal homepage: <http://www.tandfonline.com/loi/gpss20>

Dimethylsulfoxide-induced Trinuclear Co(II) and Ni(II) Salamo-type Complexes: Syntheses, Crystal Structures and Spectral Properties

Xiao-Yan Li, Quan-Peng Kang, Qing Zhao, Jian-Chun Ma & Wen-Kui Dong

To cite this article: Xiao-Yan Li, Quan-Peng Kang, Qing Zhao, Jian-Chun Ma & Wen-Kui Dong (2018): Dimethylsulfoxide-induced Trinuclear Co(II) and Ni(II) Salamo-type Complexes: Syntheses, Crystal Structures and Spectral Properties, *Phosphorus, Sulfur, and Silicon and the Related Elements*, DOI: [10.1080/10426507.2018.1452228](https://doi.org/10.1080/10426507.2018.1452228)

To link to this article: <https://doi.org/10.1080/10426507.2018.1452228>



[View supplementary material](#)



Accepted author version posted online: 13 Mar 2018.



[Submit your article to this journal](#)



Article views: 1



[View related articles](#)



[View Crossmark data](#)

Publisher: Taylor & Francis

Journal: *Phosphorus, Sulfur, and Silicon and the Related Elements*

DOI: <https://doi.org/10.1080/10426507.2018.1452228>

Dimethylsulfoxide-induced Trinuclear Co(II) and Ni(II) Salamo-type Complexes: Syntheses, Crystal Structures and Spectral Properties

Xiao-Yan Li, Quan-Peng Kang, Qing Zhao, Jian-Chun Ma, Wen-Kui Dong*

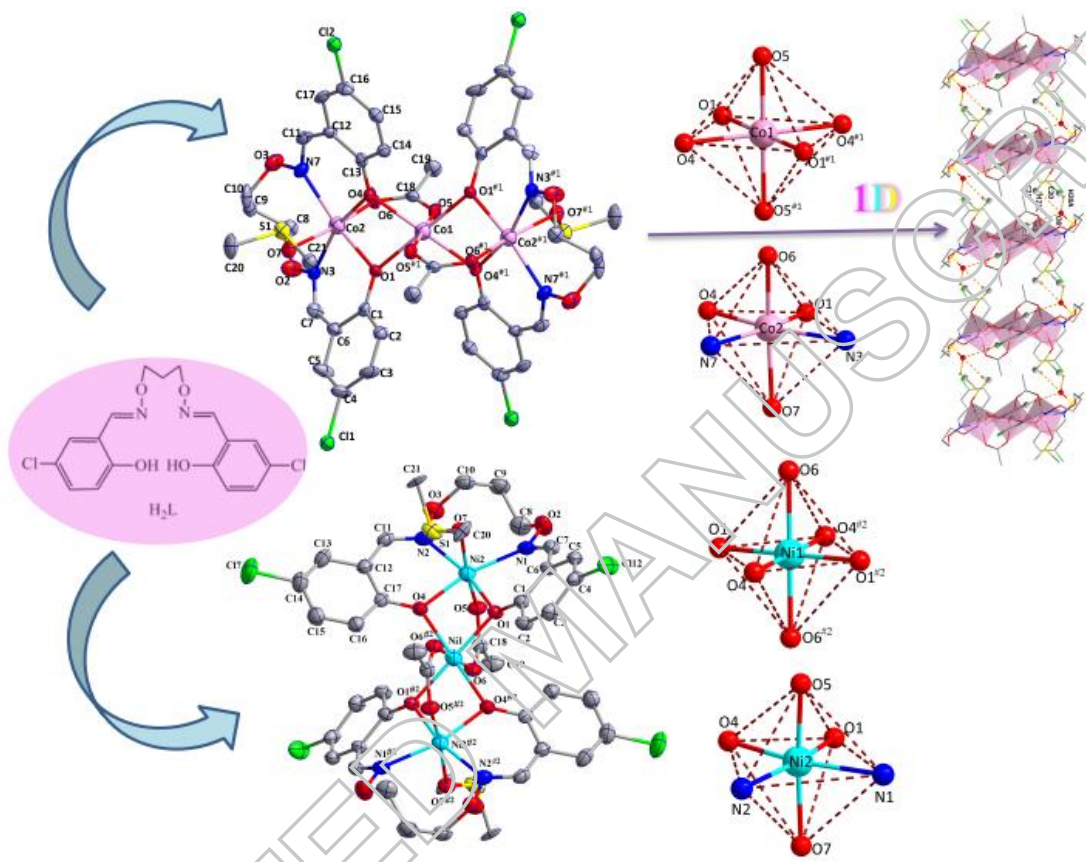
School of Chemical and Biological Engineering, Lanzhou Jiaotong University, Lanzhou,
Gansu, 730070, P. R. China

Abstract: Two homotrinuclear Co(II) and Ni(II) complexes, $\left[\{\text{CoL(OAc)(DMSO)}\}_2\text{Co}\right]\cdot2\text{DMSO}$ and $\left[\{\text{NiL(OAc)(DMSO)}\}_2\text{Ni}\right]$ have been synthesized by the reaction of 4,4'-dichloro-2,2'-(1,3-propylene)dioxybis(nitrilomethylidyne)diphenol (H_2L) with cobalt(II) and nickel(II) acetate tetrahydrate in the solution of DMSO, respectively, and characterized by elemental analyses, IR, UV–Vis spectra and X-ray crystallography. In the Co(II) complex, terminal Co^{2+} and Co^{2+} ^{#1} atoms located in the N_2O_2 sites, and are both hexa-coordinated with slightly distorted octahedral geometries. While the central Co^{2+} atom is also hexa-coordinated by six oxygen atoms, four are phenoxy oxygen atoms from two (L)²⁻

School of Chemical and Biological Engineering, Lanzhou Jiaotong University, Lanzhou, Gansu 730070, PR China.

E-mail: dongwk@126.com

units, and two oxygen atoms from μ_2 -acetate ions, which has formed a octahedral geometry. In the Ni(II) complex, coordination environments of the Ni(II) atoms are similar to those of the Co(II) atoms. Infinite 1D supramolecular structure is formed via abundant intermolecular hydrogen bonding interactions in the Co(II) complex.



Keywords: Salamo-type ligand; Trinuclear complex; DMSO molecule; Synthesis; Crystal structure

INTRODUCTION

Salen-type¹ ligands ($R-CH=N-(CH_2)_n-N=CH-R$) and their metal complexes² have been extensively investigated in modern coordination chemistry for several decades. Recently, a novel Salen-type analogue, Salamo³ ($R-CH=N-O-(CH_2)_n-O-N=CH-R$), has been developed. When an *O*-alkyl oxime unit substitutes the imine moiety, the greater electronegativity of the O atoms is predicted to improve significantly the electronic behaviors of the Salamo-type

compounds,⁴ which may give rise to novel structures and better properties of the metal(II) complexes.⁵ The novel structures of Salamo-type⁶ complexes are also fascinating, which may lead to a better potential application such as biological fields,⁷ electrochemical,⁸ catalysis activity,⁹ molecular recognition,¹⁰ magnetic materials¹¹ and luminescence properties¹² etc.

In our previous work, CH₃OH,^{6b,6d,11a} CH₃CH₂OH,¹³ CH₃CH₂CH₂OH¹⁴, CH₃COCH₃^{3f}, THF^{3e} and H₂O^{6b,12b} were involved in the Salamo-type complexes. In order to study the differences caused by the coordination of different solvents, we first studied the introduction of DMSO solvent molecules into the salamo-type complexes. Here we report two new dimethylsulfoxide-induced complexes, $[\{\text{CoL(OAc)(DMSO)}\}_2\text{Co}] \cdot 2\text{DMSO}$ and $[\{\text{NiL(OAc)(DMSO)}\}_2\text{Ni}]$. X-ray crystal structures revealed that they have similar molecular structures. In the Co(II) and Ni(II) complexes, all the Co(II) and Ni(II) atoms are hexa-coordinated with octahedral geometries.

RESULTS AND DISCUSSION

IR Spectra analyses

As shown in Fig. S 1 (Supplemental Materials), the FT-IR spectra of H₂L and its Co(II) and Ni(II) complexes exhibit various bands in the 4000–400 cm⁻¹ region. A typical C=N stretching band of the free ligand H₂L appears at 1606 cm⁻¹, while those of the Co(II) and Ni(II) complexes are observed at 1598 and 1602 cm⁻¹, respectively, which indicates that the nitrogen atoms of C=N group are coordinated to the Co(II) and Ni(II) atoms.¹⁵ Meanwhile, the free ligand H₂L exhibits Ar–O stretching frequency at 1263 cm⁻¹, while the Ar–O stretching frequencies of the Co(II) and Ni(II) complexes appear at 1201 and 1223 cm⁻¹, respectively. The Ar–O stretching frequencies of these complexes are shifted to low frequencies, which could be evidence of formation of the Co(II)–O and Ni(II)–O bonds between metal(II) atoms and oxygen atoms of phenolic groups.¹⁶

UV-vis Spectra analyses

The UV-vis spectra of H₂L and its Co(II) and Ni(II) complexes are shown in Fig. S 2. Obviously, the absorption spectrum of the free ligand H₂L consists of three relatively intense absorption peaks centered at 220, 265 and 323 nm; the former two peaks at 220 and 265 nm can be assigned to the $\pi-\pi^*$ transitions of the phenyl rings, the latter peak at 323 nm can be assigned to the $\pi-\pi^*$ transitions of the oxime group.¹⁷ Upon coordination of the ligand H₂L, the first peak of the $\pi-\pi^*$ transitions of the phenyl rings in the Co(II) and Ni(II) complexes are bathochromically shifted to 234 and 231 nm, respectively, and the second peak at 265 nm disappeared, which indicates the coordination of Co(II) or Ni(II) atoms with the ligand units, respectively.¹⁸ Compared with the free ligand H₂L, the third absorption peak at 323 nm disappears from the UV-vis spectra of the Co(II) and Ni(II) complexes, which indicates that the oxime nitrogen atoms are involved in coordination to the Co(II) and Ni(II) atoms.¹⁸ Additionally, the new absorption peaks are observed at 364 and 372 nm for the Co(II) and Ni(II) complexes, these new absorption peaks can be assigned to L→M charge-transfer (LMCT) transitions, which are characteristic of the transition metal complexes with N₂O₂ coordination sphere.¹⁹

Description of the crystal structures

The crystal structures of the Co(II) and Ni(II) complexes were determined by single-crystal X-ray diffraction. The crystal data and experimental parameters relevant to the structure determinations are listed in Table 1, and their bond lengths and angles are listed in Table 2.

Table 1 Crystallographic data and refinement parameters for the Co(II) and Ni(II) complexes.

Table 2 Selected bond lengths (Å) and angles (°) of the Co(II) and Ni(II) complexes.

Crystal structures of the Co(II) and Ni(II) complexes

The crystal structures and atom numberings of the Co(II) and Ni(II) complexes are in Fig. 1 and Fig. 2, respectively. X-ray crystallographic analysis of the Co(II) complex a trinuclear structure. It crystallizes in the triclinic system, space group *P*-1 and consists of Co(II) atoms, two completely deprotonated (L)²⁻ units, two μ_2 -acetate ions, two coordinated DMSO molecules and two crystalling DMSO molecules, which is similar to the previously reported structure of $[\{Co(5\text{-ChloroSalamo})(OAc)(THF)\}_2Co]$.^{3e} These indicate that the structures of the Co(II) Salamo-type complexes have no change when the number of carbon atoms in the alkoxy chain of Salamo-type ligand changed from two to three. In the Co(II) complex, two terminal Co(II) atoms (Co2 and Co2^{#1}) are located in the N₂O₂ coordination spheres of Salamo moieties, one oxygen atom from the coordinated DMSO molecule, the Co2 and Co2^{#1} atoms are both hexa-coordinated with slightly distorted octahedral geometries.^{6b} While the central Co(II) atom (Co1) is also hexa-coordinated by six oxygen atoms, four are phenoxy oxygen atoms from two (L)²⁻ units, and two oxygen atoms from μ_2 -acetate ions. Compared with the previously reported complexes^{3f} $[\{CoL(OAc)(CH_3COCH_3)\}_2Co]$ and $[\{CoL(OAc)(MeOH)\}_2Co] \cdot 2MeOH$, the DMSO as the solvent molecules involved in the coordination have been no reported in the Salamo-type complexes until now. Obviously, complexes informed different intramolecular hydrogen bonds. Because steric hindrance of these solvent molecules are different, the distances of Co2-O7 ($[\{CoL(OAc)(DMSO)\}_2Co] \cdot 2DMSO$), Co2-O7 ($[\{CoL(OAc)(CH_3COCH_3)\}_2Co]$) and Co2-O7 ($[\{CoL(OAc)(MeOH)\}_2Co] \cdot 2MeOH$) are 2.152(5), 2.276(2) and 2.136(5) nm, respectively. The results show that the distances between the metal and the oxygen atoms the solvent molecules are related to the steric hindrance of these solvent molecules. Structural similarities may lead to similar properties, so according to our previous reports,^{3f} the Co(II) complex may have a good antimicrobial activity.

Fig. 1 (a) View of the molecular structure of the Co(II) complex (hydrogen atoms and solvent molecules are omitted for clarity, and thermal ellipsoids are drawn at the 30% probability level). (b) Coordination polyhedra for Co(II) atoms of the Co(II) complex.

Fig. 2 (a) View of the molecular structure of the Ni(II) complex (hydrogen atoms and solvent molecules are omitted for clarity, and thermal ellipsoids are drawn at the 30% probability level). (b) Coordination polyhedra for Ni(II) atoms of the Ni(II) complex.

The corresponding interactions of the Co(II) and Ni(II) complexes are summarized in Table S 1. In the Co(II) complex, there are six intramolecular hydrogen bonds, C2–H2···O5, C8–H8A···O3, C8–H8A···O6, C10–H10A···O7, C14–H14···O1 and C21–H21A···O5. As shown in Fig. S3. The 1D supramolecular structure²⁰ (Fig. S4) of the Co(II) complex is formed by intermolecular C20–H20A···O8, C21–H21C···O8 and C15–H15···O8 hydrogen bonding interactions.

The Ni(II) complex crystallizes in the monoclinic crystal system, space group $P\bar{2}_1/c$. The single-crystal X-ray structure revealed the differences between the Co(II) and Ni(II) complexes are relatively minor. Contributions to scattering these highly disordered solvent molecules were removed using the SQUEEZE routine of PLATON. The structure of the Ni(II) complex was then refined again using the data generated.

The intramolecular hydrogen bonds of C–H···O (C2–H2···O6, C8–H8A···O3, C8–H8A···O5, C16–H16···O1 and C16–H16···O6) is present in the Ni(II) complex, and the hydrogen bonds can be seen from Fig. S 5.

EXPERIMENTAL

Materials and general methods

5-Chlorosalicylaldehyde (98%) was purchased from Alfa Aesar and was used without further purification. 1,3-Dibromopropane, other reagents and solvents were analytical grade reagents from Tianjin Chemical Reagent Factory.

Elemental analyses (C, H and N) were performed on a GmbH VarioEL V3.00 automatic elemental analysis instrument. Elemental analyses for Co(II) or Ni(II) were detected with an IRIS ER/S-WP-1 ICP atomic emission spectrometer. Melting points were obtained by the use of a microscopic melting point apparatus made in Beijing Taike Instrument Limited Company and were uncorrected. IR spectra were recorded on a Vertex70 FT-IR spectrophotometer, with samples prepared as KBr ($4000\text{--}500\text{ cm}^{-1}$). UV-vis absorption spectra were recorded on a Shimadzu UV-3900 spectrometer. X-ray single crystal structure determinations were carried out on the Bruker APEX-II CCD and SuperNova, Dual (Cu at zero) Eos four-circle diffractometers. The Supplemental Materials contains sample characterization data for the ligand and complexes (Figures S 1 – S 5, Table S 1).

Synthesis of the ligand H₂L

The ligand H₂L was synthesized according to an analogous method reported earlier.^{3f,4} (**Scheme 1**) Yield: 75.8 %. m.p. 164–166 °C. Anal. Calc. for C₁₇H₁₆Cl₂N₂O₄ (%): C 53.02; H 4.11; N 7.45. Found: C 53.28, H 4.21; N 7.31. ¹H NMR (400 MHz, CDCl₃), δ 2.14 (t, *J* = 6.0 Hz, 2H, CH₂), 4.31 (t, *J* = 6.0 Hz, 4H, CH₂), 6.85 (d, *J* = 8.0 Hz, 2H, ArH), 7.25 (s, 2H, ArH), 7.33 (d, *J* = 8.0 Hz, 2H, ArH), 8.09 (s, 2H, CH=N), 9.80 (s, 2H, OH) (Fig. S 6). IR (KBr, cm⁻¹): 3101 [ν (O-H)], 1606 [ν (C=N)], 1263 [ν (Ar-O)]. UV-Vis (CH₃OH), λ_{\max} (nm) (ε_{\max}): 265 and 323 nm (3.58×10^4 , 2.30×10^4 and 1.28×10^4 L·M⁻¹·cm⁻¹).

Scheme 1 Synthetic route to the Salamo-type bisoxime ligand H₂L.

Preparation of the Co(II) and Ni(II) complexes

Homotrinuclear Co(II) and Ni(II) complexes were synthesized by the reaction of H₂L with Co(OAc)₂ and Ni(OAc)₂, respectively (**Scheme 2**).

Scheme 2 Syntheses of homotrinuclear Co(II) and Ni(II) complexes.

A methanol solution (2 mL) of Co(OAc)₂·4H₂O (3.74 mg, 0.015 mmol) was slowly added H₂L (3.83 mg, 0.010 mmol) in DMSO (2 mL) and stirred for 0.5 h. The mixed solution was filtered, and the filtrate was kept undisturbed, several brown blocks single crystals were obtained after two weeks on slow evaporation of the solution in open atmosphere. Several brown blocks single crystals suitable for X-ray crystallographic analysis were collected and then filtration and washed with n-hexane. Yield, 3.43 mg (50.10 %). Anal. Calcd for C₄₆H₅₈Cl₄Co₃N₄O₁₆S₄ (%): C, 40.33; H, 4.27; N, 4.09; Co, 12.91. Found (%): C, 40.64; H, 4.37; N, 3.95; Co, 12.81. IR (KBr, cm⁻¹): 1598 [ν (C=N)], 1303 [ν (Ar-O)]. UV–Vis (CH₃OH), λ_{max} (nm) (ε_{max}): 234 and 364 nm (5.05×10^4 and 1.05×10^4 L·M⁻¹·cm⁻¹).

The Ni(II) complex was prepared by a similar procedure as for the Co(II) complex. Yield, 3.38 mg (49.30 %). Anal. Calcd for C₄₂H₄₆Cl₄Ni₃N₄O₁₄S₄ (%): C, 41.59; H, 3.82; N, 4.62; Ni, 14.52. Found (%): C, 41.75; H, 3.96; N, 4.47; Ni, 14.59. IR (KBr, cm⁻¹): 1602 [ν (C=N)], 1301 [ν (Ar-O)]. UV–Vis (CH₃OH), λ_{max} (nm) (ε_{max}): 231 and 372 nm (8.11×10^4 and 1.68×10^4 L·M⁻¹·cm⁻¹).

Further details of the crystal structure investigation may be obtained from the Cambridge Crystallographic Data Centre, E-mail: deposit@ccdc.cam.ac.uk on quoting the depository number CCDC–1585966 (The Co(II) complex) and 1585967 (The Ni(II) complex) contain the supplementary crystallographic data for this article.

CONCLUSIONS

In summary, two homotrinuclear Co(II) and Ni(II) complexes with a Salamo-type bisoxime ligand H₂L have been designed and synthesized. X-ray crystal structures revealed that they have similar molecular structures. In the Co(II) complex, all the Co atoms are hexa-coordinated with slightly distorted octahedral geometries. Compared with the reported complexes, this article compares and discusses the differences in the coordination of different solvents. The Co(II) complex may have a good antimicrobial activity. Furthermore, the supramolecular structure of the Co(II) complex is formed via abundant intermolecular hydrogen bonding interactions leading to a self-assembly infinite 1D chain structure.

ACKNOWLEDGEMENTS

This work was supported by the National Natural Science Foundation of China (21761018) and the Program for Excellent Team of Scientific Research in Lanzhou Jiaotong University (201706), which is gratefully acknowledged.

REFERENCES

1. (a) Sun, Y. X.; Zhang, S. T.; Ren, Z. L.; Dong, X. Y.; Wang, L. *Synth. React. Inorg. Met.-Org. Nano-Met. Chem.* **2013**, 43, 995-1000; (b) Wu, H. L.; Pan, G. L.; Bai, Y. C.; Wang, H.; Kong, J.; Shi, F. R.; Zhang, Y. H.; Wang, X. L. *J. Chem. Res.* **2014**, 38, 211-217; (c) Wu, H. L.; Pan, G. L.; Bai, Y. C.; Wang, H.; Kong, J.; Shi, F. R.; Zhang, Y. H.; Wang, X. L. *Res. Chem. Intermed.* **2015**, 41, 3375-3388; (d) Zhao, L.; Dang, X. T.; Chen, Q.; Zhao, J. X.; Wang, L. *Synth. React. Inorg. Met.-Org. Nano-Met. Chem.* **2013**, 43, 1-6; (e) Zhao, L.; Wang, L.; Sun, Y. X.; Dong, W. K.; Tang, X. L.; Gao, X. H. *Synth. React. Inorg. Met.-Org. Nano-Met. Chem.* **2012**, 42, 1303-1308; (f) Wang, P.; Zhao, L. *Spectrochim. Acta A* **2015**, 135, 342-350.
2. (a) Sun, Y. X.; Gao, X. H. *Synth. React. Inorg. Met.-Org. Nano-Met. Chem.* **2011**, 41, 973-978; (b) Sun, Y. X.; Xu, L.; Zhao, T. H.; Liu, S. H.; Liu, G. H.; Dong, X. T. *Synth. React. Inorg. Met.-Org. Nano-Met. Chem.* **2013**, 43, 509-513; (c) Chai, L. Q.; Wang, G.; Sun, Y. X.; Dong, W. K.; Zhao, L. Gao, X. H.; *J. Coord. Chem.* **2012**, 65, 1621-1631; (d) Liu, Y. A.; Wang, C. Y.; Zhang, M.; Song, X. Q.; *Polyhedron* **2017**, 127, 278-286; (e) Song, X. Q.; Liu, P. P.; Xiao, Z. R.; Li, X.; Liu, Y. A. *Inorg. Chim. Acta* **2015**, 438, 232-244.
3. (a) Dong, W. K.; Ma, J. C.; Zhu, L. C.; Sun, Y. X.; Akogun, S. F.; Zhang, Y. *Cryst. Growth Des.* **2016**, 16, 6903-6914; (b) Dong, X. Y.; Sun, Y. X.; Wang, L.; Li, L. *J. Chem. Res.* **2012**, 36, 387-390; (c) Dong, X. Y.; Kang, Q. P.; Jin, B. X.; Dong, W. K. Z.

- Naturforsch.* **2017**, *72*, 415-420; (d) Dong, W. K.; Ma, J. C.; Zhu, L. C.; Zhang, Y. *New J. Chem.* **2016**, *40*, 6998-7010; (e) Dong, W. K.; Shi, J. Y.; Xu, L.; Zhong, J. K.; Duan, J. G.; Zhang, Y. P. *Appl. Organometal. Chem.* **2008**, *22*, 89-96; (f) Li, X. Y.; Kang, Q. P.; Liu, L. Z.; Ma, J. C.; Dong, W. K. *Crystals* **2018**, *8*, 43.
4. Akine, S.; Taniguchi, T.; Dong, W. K.; Masubuchi, S.; Nabeshima, T. *J. Org. Chem.* **2005**, *70*, 1704-1711.
5. Gao, L.; Liu, C.; Wang, F.; Dong, W. K. *Crystals* **2018**, *8*, 77.
6. (a) Wang, L.; Li, X. Y.; Zhao, Q.; Li, L. H.; Dong, W. K. *RSC Adv.* **2017**, *7*, 48730-48737; (b) Dong, X. Y.; Li, X. Y.; Liu, L. Z.; Zhang, H.; Ding, Y. J.; Dong, W. K. *RSC Adv.* **2017**, *7*, 48394-48403; (c) Chen, L.; Dong, W. K.; Zhang, H.; Zhang, Y.; Sun, Y. X. *Cryst. Growth Des.* **2017**, *17*, 3636-3648; (d) Dong, W. K.; Zheng, S. S.; Zhang, J. T.; Zhang, Y.; Sun, Y. X. *Spectrochim. Acta A* **2017**, *184*, 141-150.
7. (a) Chen, C. Y.; Zhang, J. W.; Zhang, Y. H.; Yang, Z. H.; Wu, H. L.; Pan, G. L.; Bai, Y. C. *J. Coord. Chem.* **2015**, *68*, 1054-1071; (b) Wu, H. L.; Bai, Y. C.; Zhang, Y. H.; Li, Z.; Wu, M. C.; Chen, C. Y.; Zhang, J. W. *J. Coord. Chem.* **2014**, *67*, 3054-3066; (c) Wu, H. L.; Wang, H.; Wang, X. L.; Pan, G. L.; Shi, F. R.; Zhang, Y. H.; Bai, Y. C.; Kong, J. *New J. Chem.* **2014**, *38*, 1052-1061; (d) Wu, H. L.; Pan, G. L.; Bai, Y. C.; Zhang, Y. H.; Wang, H.; Shi, F. R.; Wang, X. L.; Kong, J. *J. Photochem. Photobio. B* **2014**, *135*, 33-43; (e) Wu, H. L.; Pan, G. L.; Bai, Y. C.; Wang, H.; Kong, J.; Shi, F. R.; Zhang, Y. H.; Wang, X. L. *J. Coord. Chem.* **2013**, *66*, 2634-2646.
8. (a) Dong, W. K.; Lan, P. F.; Zhou, W. M.; Zhang, Y. *J. Coord. Chem.* **2016**, *65*, 1272-1283; (b) Wang, L.; Hao, J.; Zhai, L. X.; Zhang, Y.; Dong, W. K. *Crystals* **2017**, *7*, 277; (c) Dong, W. K.; Ma, J. C.; Zhu, L. C.; Zhang, Y.; Li, X. L. *Inorg. Chim. Acta* **2016**, *445*, 140-148;
9. (a) Li, L. H.; Dong, W. K.; Zhang, Y.; Akogun, S. F.; Xu, L. *Appl Organometal Chem.* **2017**, e3818; (b) Li, X. Y.; Chen, L.; Gao, L.; Zhang, Y.; Akogun, S. F.; Dong, W. K. *RSC Adv.* **2017**, *7*, 35905-35916.

10. (a) Dong, W. K.; Li, X. L.; Wang, L.; Zhang, Y.; Dong, Y. J. *Sens. Actuators B* **2016**, 229, 370-378; (b) Dong, W. K.; Akogun, S. F.; Zhang, Y.; Sun, Y. X.; Dong, X. Y. *Sens. Actuators B* **2017**, 238, 723-734; (c) Wang, B. J.; Dong, W. K.; Zhang, Y.; Akogun, S. F. *Sens. Actuators B* **2017**, 247, 254-264; (d) Wang, F.; Gao, L.; Zhao, Q.; Zhang, Y.; Dong, W. K.; Ding, Y. J. *Spectrochim. Acta A* **2018**, 190, 111-115.
11. (a) Dong, W. K.; Ma, J. C.; Dong, Y. J.; Zhu, L. C.; Zhang, Y. *Polyhedron* **2016**, 115, 228-235; (b) Zheng, S. S.; Dong, W. K.; Zhang, Y.; Chen, L.; Ding, Y. J. *New J. Chem.* **2017**, 41, 4966-4973; (c) Zhang, H.; Dong, W. K.; Zhang, Y.; Akogun, S. F. *Polyhedron* **2017**, 133, 279-293; (d) Liu, P. P.; Sheng, L.; Song, X. Q.; Xu, W. Y.; Liu, Y. A. *Inorg. Chim. Acta* **2015**, 434, 252-257; (e) Liu, P. P.; Wang, C. Y.; Zhang, M.; Song, X. Q. *Polyhedron* **2017**, 129, 133-140. (f) Song, X. Q.; Liu, P. P.; Liu, Y. A.; Zhou, J. J.; Wang, X. L. *Dalton Trans.* **2016**, 45, 8154-8163; (g) Canaj, A. B.; Siczek, M.; Otręba, M.; Lis, T.; Lorusso, G.; Evangelisti, M.; Milioset, C. J. *Dalton Trans.* **2016**, 45, 18591-18602.
12. (a) Gao, L.; Wang, F.; Zhao, Q.; Zhang, Y.; Dong, W. K. *Polyhedron* **2018**, 139, 7-16; (b) Dong, Y. J.; Dong, X. Y.; Dong, W. K.; Zhang, Y.; Zhang, L. S. *Polyhedron* **2017**, 123, 305-315; (c) Dong, W. K.; Ma, J. C.; Dong, Y. J.; Zhao, L.; Zhu, L. C.; Sun, Y. X.; Zhang, Y. J. *Coord. Chem.* **2016**, 69, 3231-3241; (d) Wu, H. L.; Wang, C. P.; Wang, F.; Peng, H. P.; Zhang, H.; Bai, Y. C. *J. Chinese Chem. Soc.* **2015**, 62, 1028-1034.
13. (a) Dong, X. Y.; Gao, L.; Wang, F.; Zhang, Y.; Dong, W. K. *Crystals* **2017**, 7, 267; (b) Dong, W. K.; Zhu, L. C.; Ma, J. C.; Sun, Y. X.; Zhang, Y. *Inorg. Chim. Acta* **2016**, 453, 402-408; (c) Dong, W. K.; Zhang, J.; Zhang, Y.; Li, N. *Inorg. Chim. Acta* **2016**, 444, 95-102.
14. Pu, L. M.; Long, H. T.; Zhang, Y.; Bai, Y.; Dong, W. K. *Polyhedron* **2017**, 128, 57-67.
15. Dong, Y. J.; Ma, J. C.; Zhu, L. C.; Dong, W. K.; Zhang, Y. J. *Coord. Chem.* **2017**, 70, 103-115.
16. Tao, C. H.; Ma, J. C.; Zhu, L. C.; Zhang, Y.; Dong, W. K. *Polyhedron* **2017**, 128, 38-45.
17. Hao, J.; Li, L. L.; Zhang, J. T.; Akogun, S. F.; Wang, L.; Dong, W. K. *Polyhedron* **2017**, 134, 1-10.

18. (a) Ma, J. C.; Dong, X. Y.; Dong, W. K.; Zhang, Y.; Zhu, L. C.; Zhang, J. T. *J. Coord. Chem.* **2016**, 69, 149-159; (b) Li, G.; Hao, J.; Liu, L. Z.; Zhou, W. M.; Dong, W. K. *Crystals* **2017**, 7, 217; (c) Yang, Y. H.; Hao, J.; Dong, Y. J.; Wang, G.; Dong, W. K. *Chinese J. Inorg. Chem.* **2017**, 33, 1280-1292.
19. (a) Dong, W. K.; He, X. N.; Yan, H. B.; Lu, Z. W.; Chen, X.; Zhao, C. Y.; Tang, X. L. *Polyhedron* **2009**, 28, 1419-1428; (b) Wang, L.; Ma, J. C.; Dong, W. K.; Zhu, L. C., Zhang, Y. Z. *Anorg. Allg. Chem.* **2016**, 642, 834-839.
20. (a) Chai, L. Q.; Huang, J. J.; Zhang, H. S.; Zhang, Y. L.; Zhang, J. Y.; Li, Y. X. *Spectrochim. Acta A* **2014**, 131, 526-533; (b) Chai, L. Q.; Liu, G.; Zhang, J. Y.; Huang, J. J.; Tong, J. F. *J. Coord. Chem.* **2013**, 66, 3926-3938; (c) Chai, L. Q.; Zhang, H. S.; Huang, J. J.; Zhang, Y. L. *Spectrochim. Acta A* **2015**, 137, 661-669; (d) Chai, L. Q.; Tang, L. J.; Chen, L. C.; Huang, J. J. *Polyhedron* **2017**, 122, 228-240; (e) Chai, L. Q.; Zhang, K. Y.; Tang, L. J.; Zhang, J. Y.; Zhang, H. S. *Polyhedron* **2017**, 130, 100-107.

Table 1 Crystallographic data and refinement parameters for the Co(II) and Ni(II) complexes.

Complexes	Co(II) complex	Ni(II) complex
Empirical Formula	$C_{46}H_{58}Cl_4Co_3N_4O_{16}S_4$	$C_{42}H_{46}Cl_4N_4Ni_3O_{14}S_2$
Formula Weight	1369.79	1212.88
Crystal System	Triclinic	Monoclinic
Space group	$P\bar{1}$	$P\bar{2}_1/c$
$a / \text{\AA}$	9.184(2)	13.3046(12)
$b / \text{\AA}$	11.358(3)	16.1262(16)
$c / \text{\AA}$	14.494(3)	15.8073(15)
$\alpha / {}^\circ$	77.399(18)	90
$\beta / {}^\circ$	82.101(18)	95.847(9)
$\gamma / {}^\circ$	88.077(20)	90
$V / \text{\AA}^3$	1461.5(6)	3373.9(5)

Z	1	2
D _{calc} (g/cm ³)	1.556	1.194
μ (mm ⁻¹)	703	1244
Crystal size (mm)	0.34 x 0.23 x 0.21	0.33 x 0.21 x 0.19
Temp (K)	294.76(10)	295.16(10)
Theta range for collection	3.535 to 26.021	3.328 to 26.020
Reflections collected	9682	13894
Independent reflections	5728	6611
Data/restraints/parameters	5728 / 0 / 370	6611 / 0 / 326
Goodness of fit on F ²	1.026	0.906
Final R indices [I > 2σ(I)]	R ₁ = 0.0703, wR ₂ = 0.1095	R ₁ = 0.0544, wR ₂ = 0.1132
R indices (all data)	R ₁ = 0.1601, wR ₂ = 0.1606	R ₁ = 0.0923, wR ₂ = 0.1312
Largest difference peak/hole	0.996 / -0.521 e.Å ⁻³	0.640 / -0.449 e.Å ⁻³

Table 2 Selected bond lengths (\AA) and angles ($^\circ$) of the Co(II) and Ni(II) complexes.

Co(II) complex		Ni(II) complex	
Co2-O1	2.025(4)	Ni2-O1	2.034(3)
Co2-O4	2.091(4)	Ni2-O4	2.017(2)
Co2-O6	2.043(5)	Ni2-O5	2.021(3)
Co2-O7	2.152(5)	Ni2-O7	2.098(3)
Co2-N3	2.220(5)	Ni2-N1	2.151(3)
Co2-N7	2.143(5)	Ni2-N2	2.109(3)
O1-Co2-O4	79.35(16)	O1-Ni2-O4	80.60(10)
O1-Co2-O6	98.41(19)	O1-Ni2-O5	94.26(11)
O1-Co2-O7	89.83(18)	O1-Ni2-O7	91.56(10)
O1-Co2-N3	85.12(17)	O1-Ni2-N1	83.08(12)
O1-Co2-N7	163.06(18)	O1-Ni2-N2	165.00(12)
O4-Co2-O6	91.35(18)	O4-Ni2-O5	90.40(11)
O4-Co2-O7	96.85(17)	O4-Ni2-O7	97.74(10)
O4-Co2-N3	164.45(18)	O4-Ni2-N1	163.61(12)
O4-Co2-N7	84.50(18)	O4-Ni2-N2	85.47(12)
O6-Co2-C7	169.33(18)	O5-Ni2-O7	170.67(11)
O6-Co2-N3	90.2(2)	O5-Ni2-N1	89.36(12)
O6-Co2-N7	87.1(2)	O5-Ni2-N2	91.35(12)
O7-Co2-N3	83.74(19)	O7-Ni2-N1	84.11(11)
O7-Co2-N7	86.9(2)	O7-Ni2-N2	84.81(12)
N3-Co2-N7	111.0(2)	N1-Ni2-N2	110.91(14)

Figure legend

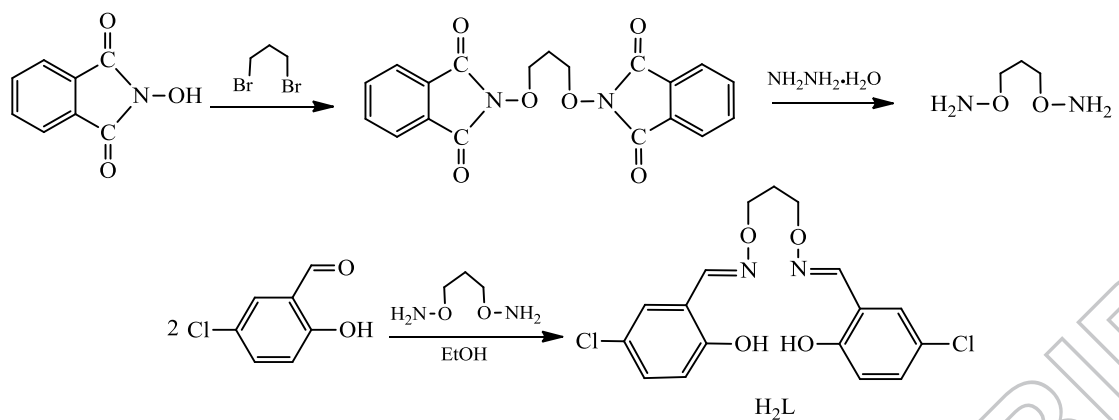
Scheme 1 Synthetic route to the Salamo-type bisoxime ligand H₂L.

Scheme 2 Synthesis of homotrinuclear Co(II) and Ni(II) complexes.

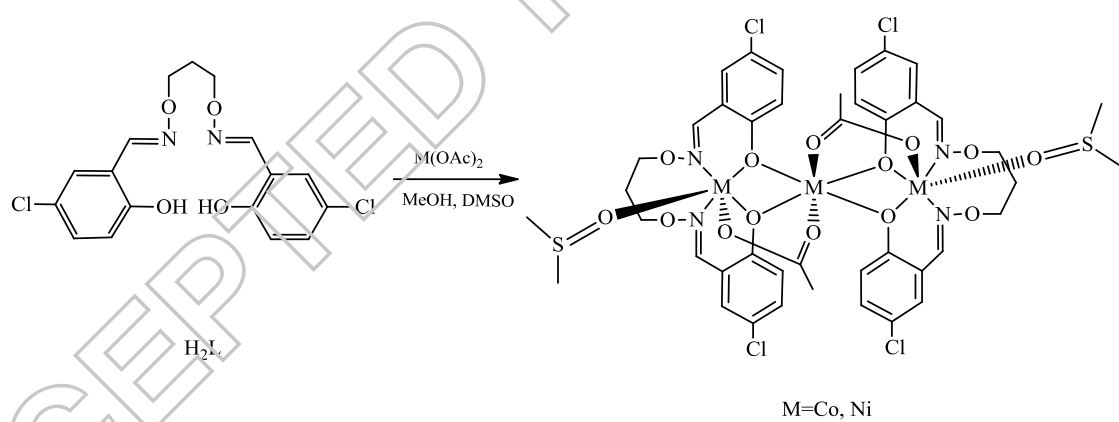
Fig. 1 (a) View of the molecular structure of the Co(II) complex (hydrogen atoms and solvent molecules are omitted for clarity, and thermal ellipsoids are drawn at the 30% probability level). (b) Coordination polyhedra for Co(II) atoms of the Co(II) complex.

Fig. 2 (a) View of the molecular structure of the Ni(II) complex (hydrogen atoms and solvent molecules are omitted for clarity, and thermal ellipsoids are drawn at the 30% probability level). (b) Coordination polyhedra for Ni(II) atoms of the Ni(II) complex.

ACCEPTED MANUSCRIPT



Scheme 1



Scheme 2

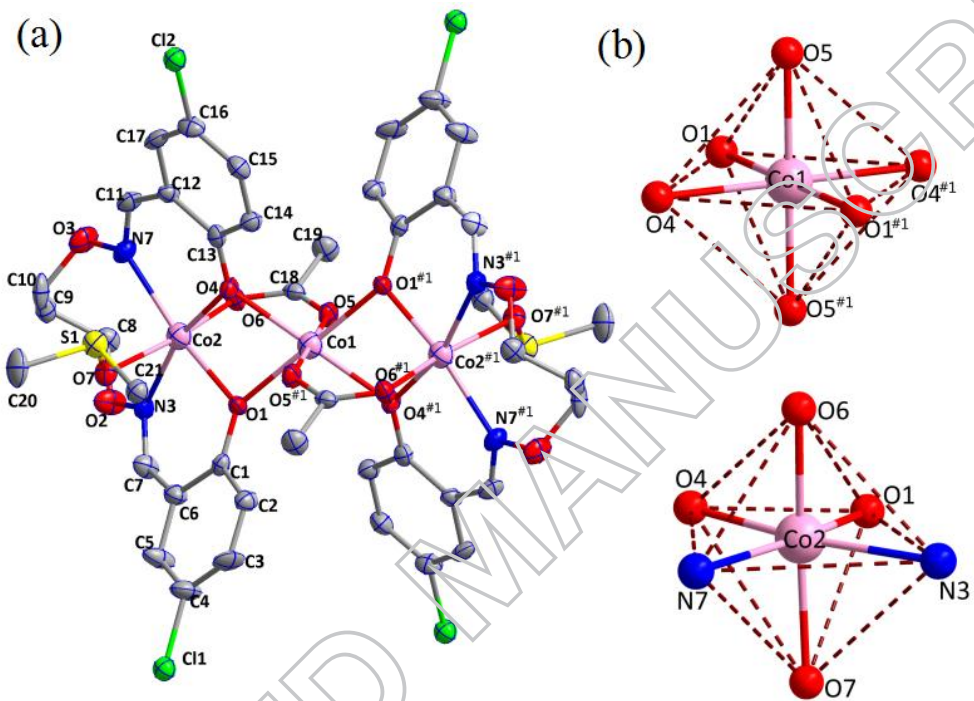


Fig. 1

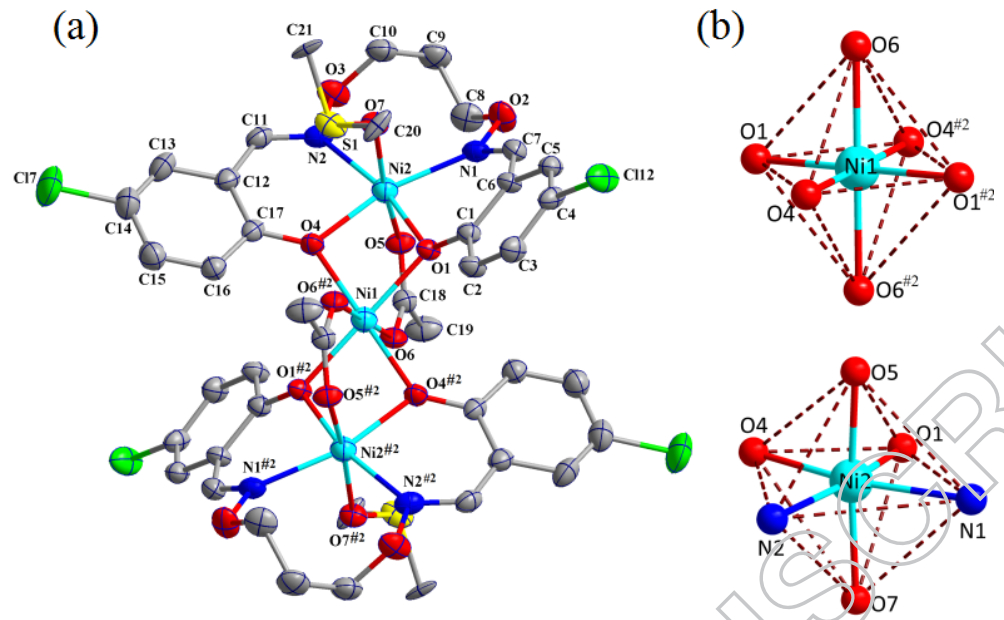


Fig. 2